JOURNAL OF MATERIALS SCIENCE 9-(1974) 369-382

Fibre-buckling in composite systems: a model for the ultrastructure of uncalcified collagen tissues

W. C. DALE, ERIC BAER
Division of Macromolecular Science, Case Western Reserve University, Cleveland, Ohio 44106, USA

Rat tail tendon and other connective tissues are being studied as unusual fibre-filled composite materials of biological origin. The collagen fibres of these tissues follow a planar wavy course along the axis of the bundle of fibres, and the straightening of this waveform produces an initial "toe region" of low modulus in the stress-strain curve, followed by a linear high-modulus region associated with stretching of the fibres themselves. Presumably this mechanical behaviour is valuable to the animal as an impact absorption mechanism.

Synthetic composite models of buckled high-modulus fibres in a soft elastic matrix have been made by differential shrinkage of the components, and show a waveform having several features in common with the collagen fibres in tendon. Both waveforms are planar, with a shape intermediate between a sine and a zig-zag. Parallel fibres buckle in phase and in parallel planes for fibre separations up to 10 diameters. When strained to high levels, both showed a previously unnoticed second waveform of smaller period superposed on the original waveform, due to slippage between the components.

A possible mechanism for fibre buckling *in vivo* is discussed.

List of symbols

D = fibre separation distance (μm).
d = fibre diameter (μm).
l_0 = half-wavelength of waveform, i.e. peak to trough distance projected on overall fibre axis (μm).
$\bar{M}_v$ = viscosity-average molecular weight (g mol^{-1})
β = angle between plane of microscope stage and plane of waveform, degrees.
ϵ = axial strain, dimensionless or percent of original length.
ϵ_∞ = strain at which waveform is just pulled straight.
ϵ_{max} = maximum strain to which sample has been subjected.
θ_0 = maximum deviation of local fibre direction from overall fibre axis, degrees.

1. Introduction

Rat tail tendon and other soft mammalian connective tissues are being studied as materials of unusual structure and mechanical properties. The major structural component of these materials is collagen, which has been recognized for some time to be organized into fibrous entities in a hierarchy of morphological levels [1]. It is also known that the collagen fibres do not lie straight along the axis of the primary tendon bundle, but follow some undulating course along it, becoming straight and parallel to the bundle axis only when the tendon is stretched. Several investigators using different techniques have described this ultrastructure variously as planar or helical, either with or without intertwining of the fibres. Recently, Diamant and co-workers analysed the waveform in rat tail tendon (RTT) in considerable detail by the straightforward technique of transmission polarizing microscopy [2], and demonstrated that the waveform is a planar shape intermediate between a sine wave and a zig-zag. They also showed how this ultrastructure gives rise to the unusual stress-strain behaviour of RTT.

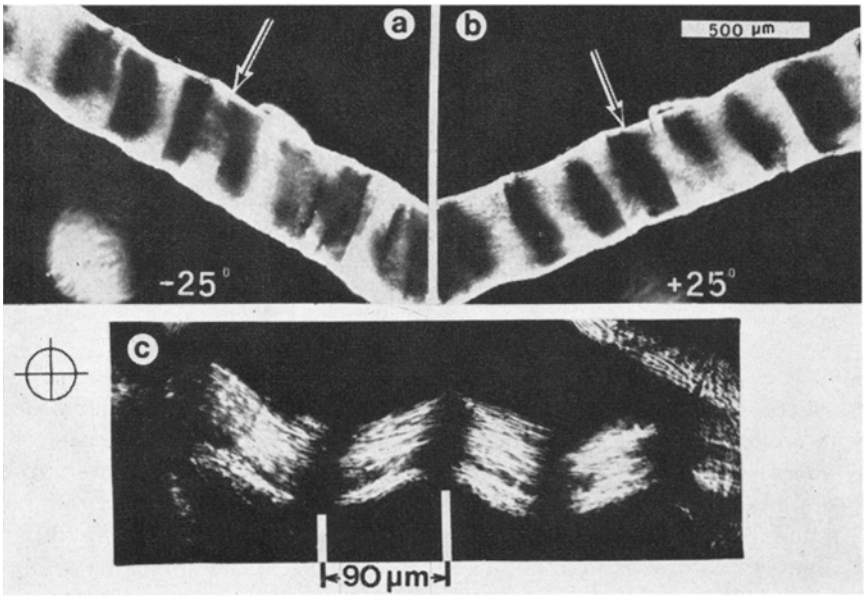

Figure 1 Ultrastructure of rat tail tendon as seen in transmitted polarized light. In (a) and (b), the intact tendon bundle shows alternating regions of transmission and extinction. Maximum contrast is seen when tendon is oriented at the angle θ_0 with respect to polarizer direction, here $\theta_0 = 25°$. Regions (arrow) which transmit at $-\theta_0$ (a) extinguish at $+\theta_0$ (b), and conversely. Scale bar 500 μm. In (c), a finely teased bundle shows the waveform physically. Extinction is seen where the local fibre direction is parallel to the polarizer direction.

Deformation in the physiological range is primarily by straightening of the waveform, analogous to the deformation of a cantilever beam under combined bending and tensile loading. The stress-strain curve shows an initial "toe region" of very low modulus, which rises smoothly into a linear high-modulus portion associated with extension of the collagen fibres themselves. Presumably this mechanical behaviour is valuable to the animal as an impact absorption mechanism, while still maintaining high ultimate strength and limited extension at unusually high loadings.

In the primary tendon bundle as pulled with forceps from the rat tail, the waveform manifests itself most clearly by alternating regions of transmission and extinction when viewed between crossed polarizers, as in Fig. 1a and b. The primary bundle, which is 100 to 500 μm in diameter, may be teased down to finer bundles, whose physical outlines follow the same waveform as that deduced from the polarizing optics of the intact primary bundle. Fibrous entities a few microns in diameter are often discernible, and these also physically follow the waveform, as seen in Fig. 1c. However, Diamant *et al*, calculated that the structural level which governs the deformation of RTT is the fibril of about 200nm diameter seen in electron microscopy, which deforms by bending.

As part of further work on the structure and mechanical properties of collagen tissues, our laboratory has reported the presence of a similar planar waveform in the collagen fibres of other mammalian tendon [3]. More recently, we have observed this waveform ultrastructure in the collagen fibres of human skin, pericardium, *dura mater*, peritoneal and other uncalcified collagen tissues (to be published), indicating that the waveform ultrastructure and the tissue mechanical properties resulting from it are quite widespread. The currently prevailing opinion on the origin of the waveform morphology seems to be that it is intrinsic to the collagen fibres, as summarized by Elliott [1]. However, Gathercole *et al* [4] have used SEM to resolve the individual collagen fibrils about 100 nm in diameter as they follow the waveform in RTT, and found that the change in direction of the fibril is accomplished without any specific changes in morphology and there is no distinguishing fine structural feature along any portion of the waveform. Also, there is significant evidence that the non-collagen components or "ground substance" [5, 6] of tendon

also play a major part in determining its properties. Partington and Wood [7] and Bychkov *et al* [9] have investigated the changes in the mechanical properties of rat tail and beef Achilles tendon respectively, using enzymatic digestions directed at the non-collagen components, and concluded that the small amounts of mucopolysaccharides and/or non-collagenous proteins in tendon were of great importance in maintaining its mechanical integrity. Related experiments in this laboratory (which will be presented in detail in a separate communication) fully support the view that the mechanical and structural properties of tendon must be considered as those of a fibrous composite material. It is useful, then, to consider the relationships between synthetic composite materials and the properties of biological composites.

Among synthetic fibre-filled composite materials, a common mode of failure in compression is by buckling of the fibres [9-11]. The shape of the buckled fibres has been treated as planar, and has been assumed [9] or calculated [11] to be sinusoidal, at least for small displacements. Buckling of synthetic fibres has also been induced without applying external stress to the composite by shrinking the matrix in which the fibre is embedded [12, 13]. Since this occurs in cooling a composite moulding, it has been referred to as thermoelastic fibre buckling, and is considered undesirable. The shape of the buckled fibre in this case has been described as helical, but in none of the above cases has there been any test to distinguish between helical and planar shapes.

The phenomenon of thermoelastic fibre buckling has not received much mechanical analysis in the literature, perhaps because it can be eliminated by appropriate selection of materials and fabrication processes. Only some rather different problems in beam buckling provide any relevant background. The buckling in compression of a free, or laterally unsupported, beam has been extensively treated; the critical stress to cause buckling, and the stresses and shape shown by a severely buckled beam are presented in standard works on elasticity, e.g. [14]. For a laterally supported beam, which is equivalent to a fibre embedded in a matrix, the critical stress for buckling has been calculated for two special two-dimensional cases: a beam on an elastic foundation [15] which considers only the compressive and bending stresses in the beam and the transverse stress in the matrix; and the uniform compression of a whole composite structure [9-11], in which the initial internal stresses are neglected. The stresses induced in buckling by differential shrinkage are more complicated than the cases treated. In the above cases, the onset of buckling has been considered incipient failure of the structure, and no consideration has been given to post-buckling behaviour or to the properties of a material containing buckled fibres.

The role of non-collagen materials in the formation of connective tissue fibres is not entirely clear, but it seems evident that interactions of collagen with the mucopolysaccharides are important [16, 17], particularly with the chondroitin sulphates [18]. Electron micrographs of collagen fibrils show them to be surrounded by a material which stains as a polysaccharide. Therefore, it seemed reasonable to question whether shrinkage of the matrix in which the collagen fibres are embedded might produce buckling of the fibres akin to the thermoelastic case described above, and produce the waveform ultrastructure of the fibres in collagen tissues. For these reasons, it was decided to use fibre buckling by differential shrinkage as the basis for developing a synthetic composite materials model for the ultrastructure of collagen tissues. A series of models was made using a variety of stiff fibres in softer matrices and different shrinkage techniques, and these were compared to the tendon samples. We have not demonstrated conclusively that fibre buckling does indeed occur in biological tissues, but there are several interesting points of similarity between the synthetic samples and the biological system, such that the possibility of fibre buckling in collagenous tissues warrants further consideration, and a preliminary description here.

2. Experimental

The fibres used were of E-glass from Owens-Corning Fiberglas, and of polycaprolactam (nylon 6) from Celanese, each of diameters 8 or 12 μm. The matrix material for the samples reported here was polystyrene (Dow Styron 690, $\bar{M}_v$ about 240 000), or poly(ethyl acrylate) polymerized *in situ*. Samples were also made using gelatin, epoxy, and various thermoplastics as matrices. These showed similar results to those reported here, but were less suitable for analysis.

The glass/polystyrene samples were cast as thin sheets, 0.5 to 0.8 mm thick. A concentrated

(40% by weight) solution of polystyrene in methyl ethyl ketone was poured into a shallow dish, the fibres were laid in, and another layer of polystyrene solution was poured on top of them. The samples were partially covered to maintain a slow drying rate which prevented the formation of a skin of hard polymer, and left in a hood for about three days while the solvent evaporated.

The nylon/poly(ethyl acrylate) samples were prepared as long cylinders about 4 mm in diameter.The fibres were suspended inside a glass tube, between hooks of 23 AWG tinned copper wire, which also kept them well centred in the tube, as shown in Fig. 2. This entire lay-up was

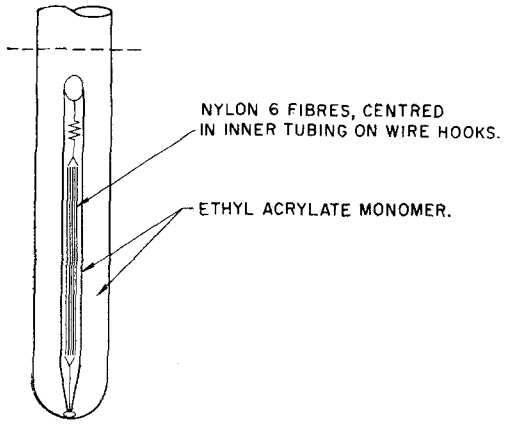

Figure 2 Schematic diagram of set-up to prepare cylindrical samples of buckled nylon fibres in poly(ethyl acrylate) matrix.

placed in an outer glass tube and monomer was added to cover the fibres. The system was frozen, evacuated, and thawed three times to remove dissolved gases, and sealed closed. Polymerization was carried out in a Cobalt 60 gamma ray source for 4 to 8 h at ambient temperatures, with a dose rate of 0.24 Mrad h^{-1}. The ethyl acrylate shrinks about 20% by volume during polymerization, and also cross links in the gamma source, resulting in a soft rubbery elastic matrix.

In both sets of samples, the modulus of the fibres was about two orders of magnitude higher than the final modulus of the matrix, but fibre buckling undoubtedly occurred while the matrix was much softer than it was in the finished sample. The shrinkage in the cast samples was primarily transverse to the axis of the fibres, and it is possible that this biased the results somewhat. However, in the polymerized cylindrical samples the fibres could usually be extremely well centred in the tube, and the matrix occasionally pulled away from the tube walls; the shrinkage, therefore, was definitely symmetric about the fibre axis, and probably near to isotropic in the central portions of the samples.

Optical observations were made with a Reichert Zetopan microscope, using transmitted polarized white light. The cylindrical samples showed considerable lens effect, and when this interfered with observations, it was reduced by immersing the samples in water. A rotating disc compensator with combination plates of quartz was used for the measurements of optical path difference, using standard techniques, e.g. [19].

3. The buckling of single fibres

A single buckled nylon fibre in a poly(ethyl acrylate) matrix is shown in Fig. 3 at various angles, θ, between the polarizer direction and the gross fibre axis. In these micrographs, the polarizer and analyser directions are approximately horizontal and vertical in the frame of the photographs. Fig. 3a shows the fibre with the polarizers fully crossed, and Fig. 3b shows the shape of the fibre as viewed with no polarizers. Extinction is seen where the local direction of the fibre coincides with the polarizer direction, i.e. at the apices of the waveform when the gross fibre axis is along the polarizer direction. The rest of Fig. 3 was taken with the polarizers not quite crossed, so that both the fibre itself and the extinction bands can be discerned. As the microscope stage is rotated, alternate extinction bands approach each other and merge until a position is reached where there is maximum contrast between the transmitting and extinguishing portions of the fibre. This is referred to as the θ_0 position, which denotes the maximum angular deviation of the local fibre direction from the gross fibre axis. The value of $\theta_0 = 28°$ for the fibre in Fig. 3 is at the upper end of the range found in tendons. Rotation beyond the θ_0 position results in decreased contrast, until at $\theta = 45°$, the fibre shows maximum transmission all along its length. This is precisely the optical behaviour of RTT from which Diamant *et al* [2] deduced the presence of the waveform before its physical shape was observed. The behaviour shown in Fig. 3 of this paper corresponds in detail to Diamant's Figs. 1, 2, and 8 for the intact tendon bundles, schematic drawing, and teased tendon bundles, respectively.

The result of rotating a buckled fibre sample about its own gross fibre axis is shown in Fig. 4.

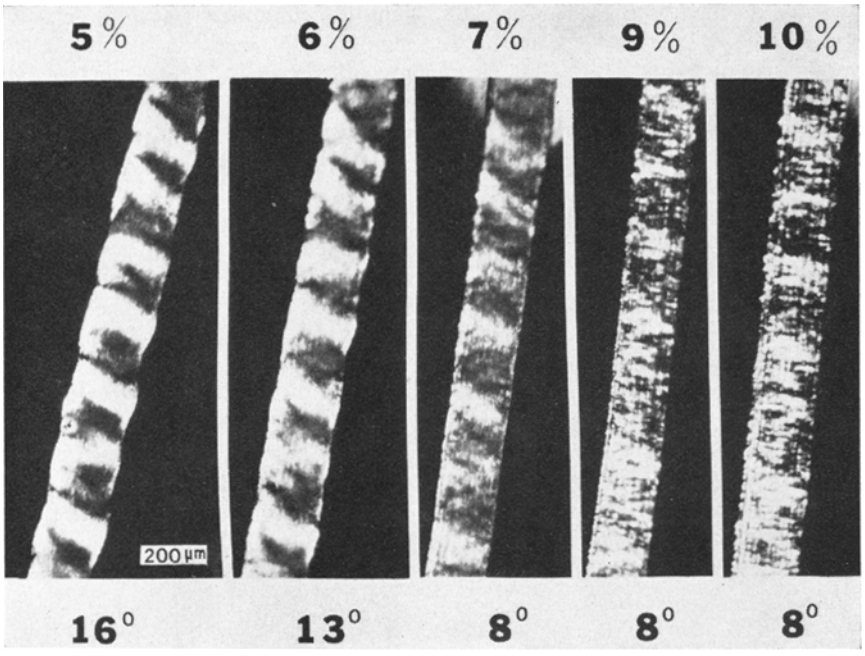

Figure 3 Behaviour of extinction bands as single buckled nylon fibre is rotated with angle shown between the overall fibre axis and the polarizer direction. In (a) polarizers are fully crossed; in (b) they are parallel; in the rest, polarizers are not quite crossed to show both physical shape and optical behaviour of the fibre.

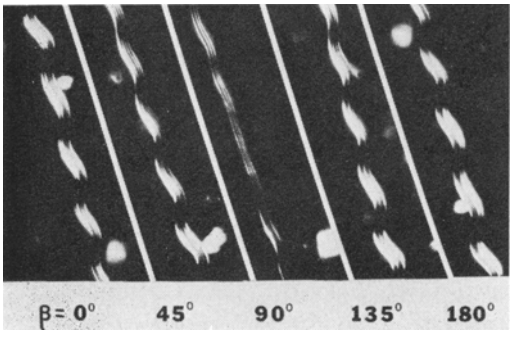

Figure 4 Buckled nylon fibre sample rotated about the overall fibre axis by the angle indicated. β denotes angle between the plane of the waveform and the plane of the microscope stage.

In Fig. 4a, the fibre was placed in its θ_0 position, here $\theta_0 = 15°$, and simultaneously rotated about the cylindrical axis of the sample until the waveform was seen most clearly, which is taken as the $\beta = 0$ position. As the sample is further rotated about its own axis by the angle β, the apparent amplitude of the waveform and the contrast between transmitting and extinguishing regions of the sample both decrease until at $\beta = 90°$, they both reach a minimum. As the sample is rotated beyond $\beta = 90°$, contrast reappears, but regions which appeared dark at angles $0 < \beta < 90°$ transmit at angles $90° < \beta < 180°$ and conversely. At $\beta = 180°$ there is full restoration of contrast and amplitude. Clearly, the waveform of the buckled fibre is planar as opposed to helical, and the positions $\beta = 0$ and $\beta = 90°$ correspond to looking straight down upon, and along the plane, respectively. Fig. 4 shows, in fact, the manipulation devised by Diamant *et al* to distinguish between planar and helical waveforms in tendon, and duplicates the results shown in Fig. 5 of their paper on rat tail tendon. The minimum in contrast separating a sharp reversal of transmitting and extinguishing regions is sufficient to show planarity; it is helpful but not necessary to be able to see the waveform physically.

Although the cylindrical samples were very convenient to demonstrate that the buckled fibres were in a planar shape, this could also be determined in the sheet samples with only slightly less certainty. The × 10 objective lens of the microscope had a focal depth of field of about 10 μm, and the displacement of the fibre relative to an arbitrary datum plane could be determined to about this precision by noting the amount of

vertical stage travel needed to preserve focus as different parts of the waveform were scanned. Of the several dozen cylindrical and sheet samples examined, some showed more departure from planarity than that shown in Fig. 4, and some showed less, but in no case did the waveform of the buckled fibres resemble the helical shape previously suggested in the literature.

4. Geometry of buckled fibres

Although the simplest shape for a planar waveform would be a sine wave, it was noted by Diamant *et al* [2] that the shape of the waveform in rat tail tendon was instead intermediate between a sine wave and a planar zig-zag, as may be noted in Fig. 1c. It is also known that the shape of a buckled free beam, that is one which is not laterally supported, is strictly sinusoidal only in the limit of infinitesimal displacements. The shape for the case of large displacements is

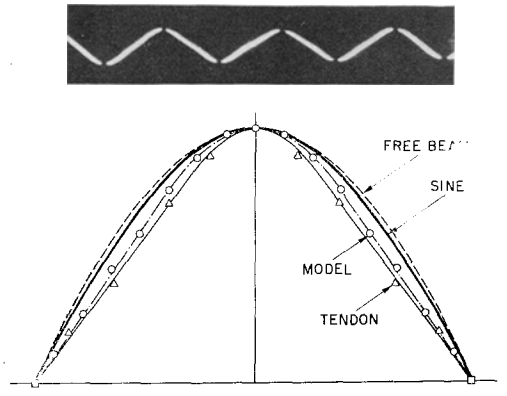

Figure 5 The shape of the waveform in the buckled fibre models compared to that of rat tail tendon. The shape of a pure sine wave and of a buckled free beam are shown for reference.

available in texts on the theory of elasticity, e.g. [14], as the problem of the "elastica".

The shapes of several buckled fibre samples were plotted and compared to sine waves of the same amplitude and periodicity. While some of the samples could reasonably be described as sinusoidal, many samples, especially those showing large values of θ_0, showed very definite deviations from this shape, and the deviation was always toward the shape of a zig-zag. Fig. 5 shows the shape of such a zig-zag buckled fibre and compares its shape to that of the waveform in RTT as shown in Fig. 1c, to a pure sine wave, and to a buckled free beam, all reduced to the same amplitude and half-wavelength. It is seen that the shapes of the buckled fibre model and of tendon are quite similar, while the free beam which is not surrounded by a matrix material shows entirely the opposite type of deviation from the sinusoidal shape, and becomes more broadly bowed. The difference in shape between the buckled fibre model and the free beam must be attributed, then, to the presence of the matrix, and implies that the presence of a matrix also influences the shape of the waveform in RTT similarly.

5. Double- and multiple-fibre interactions

For the case of a uniformly compressed composite material, there are two simple relationships possible between adjacent fibres [9-11]. The

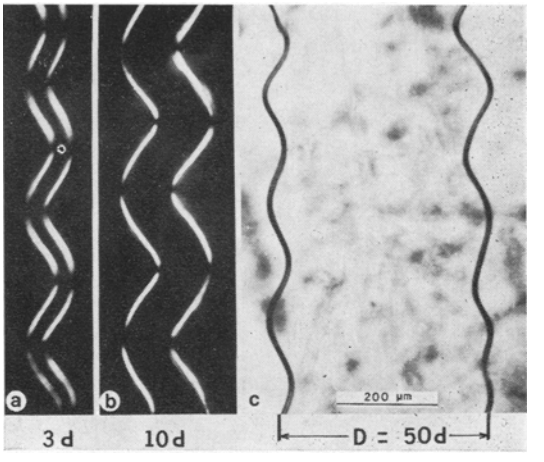

Figure 6 Co-operative buckling between double fibres. Parallel fibres buckle only in phase at separations up to 10 diameters (a) and (b). Only at very large separations above 50 diameters (c) do they buckle independently.

fibres may buckle all in phase (shear mode), or with alternate fibres out of phase by one-half cycle (extension mode). Where the volume fraction of the fibres is below about 0.3 the extension mode prevails, and the shear mode is dominant at higher fibre fractions. While mature tendon contains collagen fibre fractions upwards of 0.6, developing young tendon shows a fibre fraction which is in the range of 0.3 [20, Fig. 23 in 17], and is probably even smaller in the earliest stages of fibre formation.

For the present samples, fibres buckled by the differential shrinkage method showed only the in-phase (shear mode) relationship for fibre

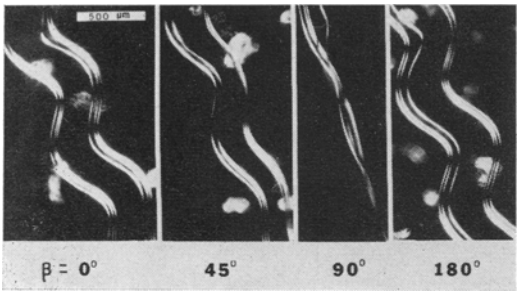

Figure 7 Co-operative buckling among multiple fibres in two groups of three, separated by about 20 fibre diameters. The sample is rotated about the overall fibre direction. The waveform of each individual fibre is planar. The planes of the waveforms of the set of fibres are all parallel, and in this case coincide with the plane defined by the original centrelines of the set of fibres. β denotes angle between plane of the buckled fibres and plane of the microscope stage.

separations up to 10 diameters or more, as shown for samples of two fibres in Fig. 6a and b. Only at fibre separations of about 50 diameters or more was the buckling of two parallel fibres clearly non-co-operative, as shown in Fig. 6c. At separations intermediate between 10 and 50 diameters, other possible relationships between buckled fibres were observed, but there were insufficient samples in this range to decide whether these were truly co-operative relationships or only happenstance. Samples with more than two fibres seemed to show co-operative effects for even greater separations.

The relationship between the planes in which the individual fibres buckled is shown in Fig. 7, where the sample contain six fibres in two groups of three separated by about 20 diameters. When the sample is rotated about the gross fibre axis, it is seen that the fibres buckled co-planar, in the plane defined by the centrelines of the unbuckled fibres. The relationship was again the only one observed for fibre separations less than about 10 diameters. Multiple planes of fibres were not specifically investigated, but for arrays where the fibre centrelines were not originally in the same plane, the planes in which the individual fibres buckled were all approximately parallel, and the waveforms still in phase, for fibre separations up to at least 10 diameters. Thus the waveform of the synthetic samples corresponded in detail to that of the collagen fibres in RTT and other collagen tissues, even for very low fibre fractions.

6. Strain field in the matrix surrounding fibre

Little could be observed of the strain field in the rubbery matrices, although the brightening of the background in Fig. 3 as θ increased from 0° to 45° shows an overall strain in the matrix. Nor is any information accessible about the strains in the ground substance of connective tissue. The polystyrene matrix, however, showed information of this kind in some detail. For this section, samples were selected for which the plane of the buckled fibre corresponded approximately to the plane of the cast sheet. The birefringence around a single buckled glass fibre in polystyrene is shown in Fig. 8a. The first point of interest is that the matrix shows significant birefringence at distances in excess of 450 μm from the fibre, or about 40 fibre diameters. Secondly, one notes that there are also alternating regions of extinction and transmission in the matrix as one scans along the fibre. However, as the sample was rotated about the normal to the plane of the buckled fibre, the motion of the extinction regions in the matrix was quite different from that caused by the birefringence of the fibre itself. In the $\theta = 0$ position, the extinction regions are at the apices of the waveform in both the fibres and the matrix. As the sample is rotated, the extinction regions translate along the fibre, and no longer are continuous across it, except where θ is 45° or multiples thereof.

The optical path differences (OPD) measured with the quartz compensator were rather small, the larger being in the range 10 to 30 nm for various samples, with a subjective error in locating the extinction position of about 2 to 3 nm. All measurements were left in the form of OPD, since it was not possible to assess the effective thickness of the strained regions. The magnitude of the OPD in the matrix adjacent to the buckled fibres did not show much variation at different points along the waveform. However, the transmission directions have a periodically varying orientation with respect to the overall fibre direction as one scans along the waveform as sketched in Fig. 8b. Unfortunately, the OPD indicates only the difference between the algebraically largest and smallest strains, and not the actual magnitude of either.

Interpretation of the strain becomes clearer when a double fibre sample is examined, as in Fig. 9. In Fig. 9a, areas between the fibres and outside them both show the same alternation of transmitting and extinguishing regions, indicating

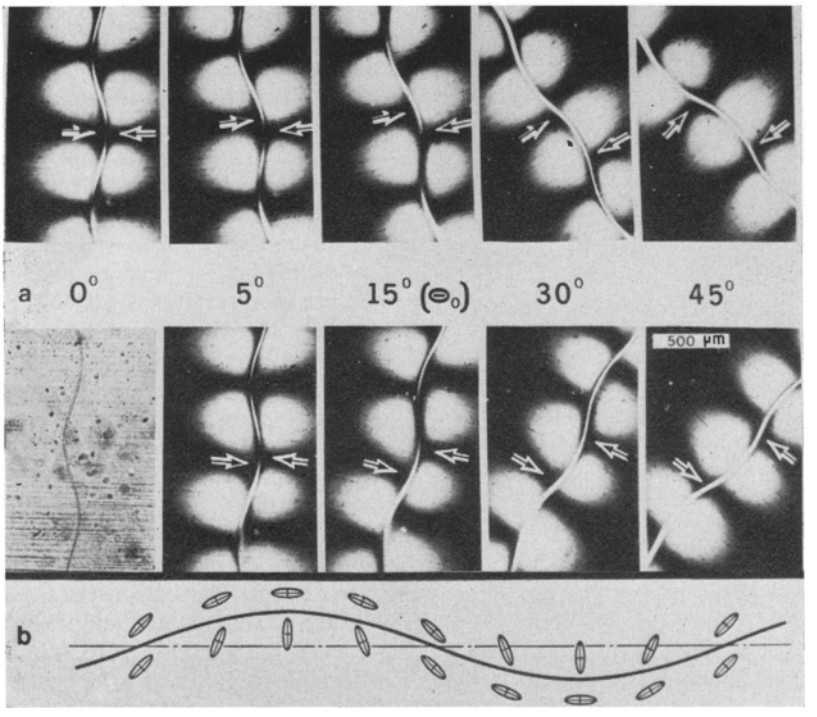

Figure 8 (a) Strain field in the polystyrene matrix around a buckled glass fibre. As the microscope stage is rotated with respect to the polarizers by the indicated angle, the extinction pattern in the matrix shifts in quite a different way from that in the fibres, as described in text. Arrow denotes the same extinction region in each photograph. (b) Schematic diagram of birefringence field in matrix. Long axis of ellipse denotes faster transmission direction.

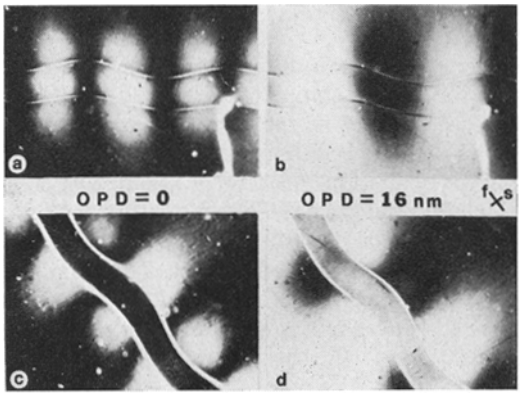

Figure 9 Strain field in the polystyrene matrix of double glass fibre sample. No compensator used in (a) and (c). In (b) and (d), compensator setting corresponds to 16 nm optical path difference, and the faster optic axis (i.e. lower refractive index direction) of the sample is oriented NW-SE in the frame of the photographs.

periodic fluctuation in the magnitude of the shear strain perpendicular to the overall fibre direction. When the compensator was used to extinguish this birefringence, as in Fig. 9b, it was seen that: the magnitude of this shear strain was greatest at the nodes; was approximately the same between the fibres and outside them; and the sign at the nodes where the local fibre direction showed a positive slope was opposite from that at the nodes where the fibre had a negative slope, all as might be expected. In Fig. 9c, the sample is rotated by 45° and shown with no compensator. The matrix outside the fibres shows regions of transmission at the apices of the waveform, but the region between the fibres is fairly uniform and not far from extinction. Thus there are significant strains parallel or perpendicular to the overall fibre axis in the matrix outside the fibres, but not in the matrix between fibres. When the birefringence was compensated, as in Fig. 9d, extinction was seen in the matrix outside the fibres on the convex side of the apices, corresponding to compression transverse to the fibre direction at these points. The region between the fibres is not quite uniform, but the variations are too small to measure. When the sample was rotated by 90°, extinction was seen on the concave sides of the apices, indicating transverse tension at these points.

The major strains seen in the matrix, then, are the lateral restoring strains which oppose the transverse displacement of the fibre, and the shear strains which oppose the rotation of the local fibre direction away from the overall fibre axis. The former are reduced in the area between fibres which are close together.

7. Deformation behaviour

The synthetic models reproduce the essential geometric features of the collagen ultrastructure described by Diamant *et al*; we consider now their behaviour during deformation. The models described here did not show a significant "toe region" in their stress-strain curves, as the biological tissues do, although a reason for this is readily apparent. In the present models, which are rather preliminary, buckling occurred while the matrix was still very soft, and the matrix hardened considerably further before the samples were suitable for handling. As a result, the stress-strain curves were dominated by the strength of the matrix material, and were essentially Hookean. In the biological systems, however, the sequence of events would be quite different. If fibre buckling does occur, it would happen during the earliest stages of fibril formation, as will be discussed later. Radial growth of the fibril is by deposition of additional collagen on an already deformed substrate; the collagen stiffens by cross-linking while the amount of matrix material decreases. Thus the stress-strain behaviour of tendon is dominated by the straightening of the waveform, as described by Diamant *et al* [2].

However, in both the biological and the synthetic materials larger deformations cause other effects on the ultrastructure which have not been reported previously.

7.1. Biological tissues

It is generally known that the collagen fibres in tendon become straightened out when the tendon is strained, and the waveform reappears on unloading if the strain is not too large. At strains above this elastic limit, irreversible changes are seen in the stress-strain curves, and it has been reported that the waveform disappears and never returns [21, 22]. We have observed, however, that instead of disappearing the waveform may be altered greatly in size.

In examining the effects of chemical treatments on the reversibility of the stress-strain curves and of the waveform, we have used the technique of incremental strain cycling, i.e. the sample was extended and then returned to its original length at a constant rate, and the maximum strain was increased by a fixed increment for each successive cycle. For the results shown, the strain increment was 1%, and the strain-rate was 10% min^{-1}. In agreement with other workers, we find that the waveform and the stress-strain curves are essentially reversible for strains within the "toe region" associated with straightening of the waveform, and into the linear region of the stress-strain curve. The effect of higher maximum strains on the waveform is shown in Fig. 10. For the sample shown, ϵ_∞, the strain at which the waveform was just pulled straight, was 3.5%, and after strains to $\epsilon_{max} = 4$ and 5%, there was no change in the appearance of the sample after it was unloaded. Strains to ϵ_{max} of 6 and 7% each produced a decrease in the θ_0 angle, and reduced the contrast visible in the waveform. Strains to 8, 9 and 10% ϵ_{max} did not result in pulling the fibres permanently straight, however, but resulted in the appearance of a new waveform which was superimposed on the original one, and in some cases obliterated the original one entirely. The new waveform was of much smaller periodicity than the original, though the wavelengths did not seem to be numerically related. In Fig. 10, the original waveform has a half-wavelength, denoted l_0, of about 110 μm, and the small-period waveform is about 20 μm; waveform less than 5 μm has been induced by strain cycling. The possibility was considered that light and dark striations in the samples might be due to other causes, but the movement of the extinction regions as the microscope stage was rotated corresponded exactly to that shown in Fig. 3, demonstrating that this was indeed a new waveform. There was no tendency for the waveform to revert to its original size on prolonged storage under no load.

The new small-period waveform was seen most clearly in tail tendons from young rats (e.g. two months as in Fig. 10) which had been incrementally strain cycled, but it was also seen in mature RTT (6 months) strained monotonically to break, especially near the fracture site. Only in very old rats was it questionable if the phenomenon occurred. The range of strains in which small-period waveform appeared corresponded to stress-strain curves which showed pronounced reductions in modulus from the earlier cycles, and an increase in the length of the toe region. No small-period waveform was

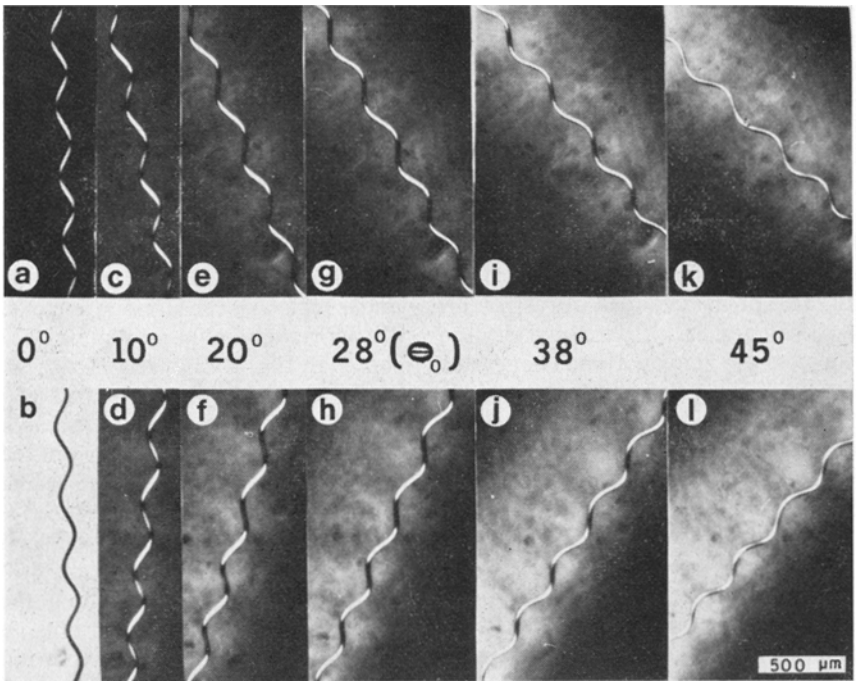

Figure 10 Development of small-period waveform in rat tail tendon. Sample was extended to strain indicated above each photograph, then unloaded, photographed, and strained to next highest level. Optimum contrast angle θ_0, indicated below each photograph, does not decrease to zero, but a much smaller waveform appears in the tendon, superposed on the original.

seen in RTT cycled extensively to strains below that needed to completely straighten the waveform, or below the elastic limit.

It is possible that a similar reduction in size of the waveform occurs *in vivo* in tendons subject to high strain, load bearing or impact requirements. For example, human Achilles tendon, which would be expected to have higher load bearing requirements *in vivo* than rat tail tendon, is also characterized by a much smaller l_0 and θ_0 than RTT [3]. The characteristics of the waveform produced artificially in RTT by strain cycling *in vitro* are quite similar to those of human Achilles tendon.

7.2. Synthetic models

The synthetic composite systems also showed a great reduction in the period of the waveform when they were strained to sufficiently high levels. The waveform of the buckled fibres was observed to straighten out as the samples were strained, as expected, and this was reversible for small strains. Samples were strained manually beyond the point where the fibres were completely straightened, and the effect on the waveform after unloading the samples is shown in Fig. 11. Again a second waveform of smaller period was superposed on the original one.

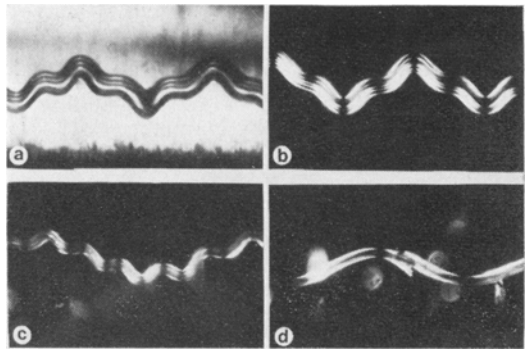

Figure 11 Development of small-period waveform in nylon/poly(ethyl acrylate) models, strained beyond elastic limit. In (a) and (c), small-period waveform appears superposed on the original. In (d), the fibre has fractured (which was rare), and there is no small-period waveform.

In the case of the synthetic samples, the mechanism by which the small-period waveform was formed is fairly clear, and is shown in Fig.

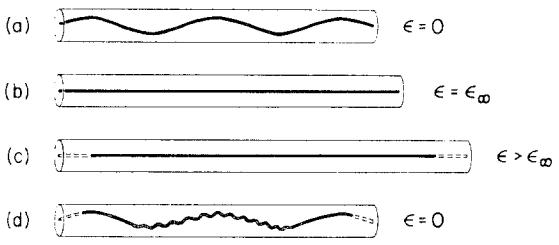

Figure 12 Schematic diagram of mechanism by which small-period waveform develops in models, described in text.

12. The samples could be strained without internal damage from $\epsilon = 0$ (Fig. 12a) to ϵ_∞ (the strain at which the fibres were just pulled straight, Fig. 12b), and just slightly further. At higher strains, the samples failed by slippage at the interface between the fibres and matrix, since no particular steps were taken to assure adhesion. The rubbery matrix continued to extend while the much stiffer fibre stayed at a constant and smaller strain, slipping within the channel of matrix material (Fig. 12c). In several samples, the free ends of the fibres, which were originally flush with the ends of the sample, were observed to have withdrawn into the sample, leaving an empty channel behind. As the sample was released, the buckled fibre rebuckled within the channel in the matrix material as a means of accommodating the increased strain differential between the fibres and matrix, resulting in the small-period waveform shown in Fig. 11a to c. Only very rarely was the interface strong enough to cause fracture of the fibre, as shown in Fig. 11d. Here, the broken ends have also returned to their original positions.

The above mechanism implies that rebuckling would be most favoured in the central portion of the sample length where the compressive stress on the fibre was greatest and the shear stress on the interface was least, and similarly rebuckling would be least favoured at the ends of the fibres. In the samples examined, rebuckling was observed over most of the length of the fibre, but not in the segment near free ends (as indicated in Fig. 12d), nor near ends created by fibre fracture (Fig. 11d). If only the transverse stresses in the matrix and the compressive and bending stresses in the fibre are considered, the present samples may be analysed as a beam on an elastic foundation [15]. Using the fibre properties and geometry of the present samples, this analysis predicts a critical stress for rebuckling of 2000 to 5000 psi,* which is at least one order of magnitude smaller than the fracture stress in tension.

Because the small-period waveform in rat tail tendon occurs only when the tendon is strained beyond its elastic limit, and in monotonically strained samples is seen most clearly near the fracture site, it is clearly associated with slippage between the collagen fibres after the medium transferring stress between the fibres has failed. The analogous phenomenon of fibre rebuckling in the synthetic samples is much more readily understood, and may offer a starting point for understanding the failure mechanism of tendon. However, the identification of the entities in tendon corresponding to the fibre-matrix interface and to the pre-existing channel is far from obvious.

8. The prospects for fibre buckling in biological systems

The synthetic models based on fibre buckling accurately reflect several important features of the waveform ultrastructure of fibrous collagen tissues, as summarized in Table I. Reproduction of the geometric features is quite good, and both types of materials show a planar waveform of comparable shape and the same co-operative relationships between multiple fibres. The models reproduce only some features of the deformation behaviour of the tissue such as straightening of the fibres and the small-period waveform. The differences in the stress-strain curves are probably due to excessive hardening of the matrix after fibre buckling has occurred in the models, and by improving fabrication procedures it is most likely that these differences could be essentially eliminated. It is natural to inquire whether the models are only phenomenologically similar to the tissues, or whether fibre buckling also occurs in biological systems. However, to date no critical experiment has been conducted which answers the questions decisively.

It has long been known that skin wounds involving loss of substance do undergo lateral contraction during the generation of new tissue [23], but the relation of this fact to the waveform in the collagen fibres of skin is not yet clear. It is necessary, then, to consider what is known about the interactions between collagen and the

*10^3 psi = 6.89 N mm^{-2}.

TABLE I Summary comparison of ultrastructural features of rat tail tendon, and fibre-buckling models

Rat tail tendon	Models
1. Planar waveform	√ as in tendon
$\theta_0 = 7°$ to 30°	√ as in tendon
$l_0 = 20$ to 100 μm*	quite variable
$d = 100$ nm, $l_0/d = \sim 500$*	$d = \sim 10$ μm, $l_0/d = 10$ to 100
2. Shape intermediate between sine and zig-zag	√ as in tendon
3. Fibres in phase	√ for D/d up to 10
4. Planes of waveform parallel	√ for D/d up to 10
5. Deforms by fibre bending	unknown
6. Toe in stress-strain curve	NO, matrix stiffness dominates
7. Develops small-period waveform	√ mechanism understood
8. Matrix stresses important	√ suitable for study of matrix stresses

*These are typical values in RTT 2 weeks to 3 months old, but corresponding values for embryonic tendon are not available.

ground substance of connective tissue, and inquire whether a means for fibre buckling may occur *in vivo*. In tendon, the structural components of the ground substance matrix consist of: the mucopolysaccharides hyaluronic acid, chondroitin sulphates B and C; and non-collagen protein, at least some of which is bound to the mucopolysaccharides [6, 24, 25]. The mucopolysaccharide composition varies from one connective tissue to another, but the mixture of hyaluronic acid and some chondroitin sulphates is quite widespread, and the following discussion will be in terms of these two classes of polysaccharides, and the differences in their properties. Alternative discussions in terms of non-collagen protein components, elastic fibres, or even cellular changes might be envisioned, but these are not at all clear at present, and are even more hypothetical.

The chondroitin sulphate-proteoglycan (CS-P), usually obtained from cartilage, interacts strongly with collagen. Addition of CS-P to tropocollagen solutions under approximately physiological conditions causes rapid gelation or precipitation of collagen fibrils in native form [18, 26]. Lowering the temperature to 4°C suppresses growth of the fibrils, but nucleation of them still occurs instantaneously. CS-P is generally recognized to consist of a number of chondroitin sulphate side chains attached to a central protein core [25, 26], and these in turn may form larger aggregates [27]. If the protein is removed, the individual protein-free CS chains still interact strongly with individual tropocollagen or polypeptide molecules, forming a complex with calfskin tropocollagen seen by electrophoresis [26], causing a major change in the conformation of polylysine [28], and raising the thermal denaturation temperature of tropocollagen from 38 up to 46° C [29]. However, protein-free CS is of relatively little effect in promoting aggregation of tropocollagen into fibrils [18]. Apparently multiple points of contact between several tropocollagen molecules and several CS chains of the CS-protein are necessary to promote nucleation, and the CS-P plays a significant role in stabilizing the fibril. On the other hand, hyaluronic acid shows much weaker interactions than chondroitin sulphate in the nucleation of fibril aggregates [18], and in stabilizing tropocollagen against thermal denaturation [29].

The mucopolysaccharides largely determine the volume of the connective tissue matrix and any possible changes in that volume, since they are highly hydrated *in vivo*. The mucopolysaccharides as a class show major space-filling or excluded volume effects, in that when in solution they immobilize or exclude to other molecules a much larger volume of solution than just the volume of the dry polysaccharide molecules. Of the mucopolysaccharides as a class, however, hyaluronic acid shows these effects most pronouncedly [25, 30]. *In vivo*, hyaluronic acid frequently serves a space-filling or lubricating role, as in the vitreous body of the eye or in synovial fluid. Hyaluronic acid may play a role in reducing the flow of water and regulating the passage of smaller molecules through the connective tissue ground substance, as has been discussed extensively by Laurent [30].

Conditions for fibre buckling *in vivo* would be most favourable when the ratio of polysaccharide ground substance to collagen is greatest, which is during fibre formation. Fitton Jackson [20] found collagen volume fractions of

0.2 to 0.3 in embryonic chick metatarsal tendon. The fibre fraction was increasing rapidly at this stage of development, and since the collagen fibres were first distinguished when their diameters were about 8 nm, it is likely that the earliest stages of development involve still smaller collagen fibres and smaller fibre volume fractions. Also, the waveform ultrastructure is clearly visible in tail tendon from rats as young as newborn. In injured tails of old rats, the new fibres formed in the healing wounds have been observed to have the ultrastructure characteristic of young rat tail tendon, i.e. the waveform is related to the time elapsed since formation of the collagen fibre, rather than to the calendar age of the animal [2]. It is also during fibre formation that the concentration and metabolic turnover of the polysaccharides is highest.

The two classes of connective tissue polysaccharides, then, serve essentially different functions; chondroitin sulphates play an important structural role in fibre formation and probably some space-filling role, while hyaluronic acid plays predominantly a space-filling role and perhaps only a minor structural role. The relative turnover rates and concentrations of the connective tissue polysaccharides have been reviewed extensively by Sobel [6], who noted that hyaluronic acid shows a considerably higher metabolic turnover rate than the chondroitin sulphates in several tissues, and responds more rapidly in repairing tissue trauma. There is a general pattern shared by a number of tissues, consisting of a decreasing concentration of mucopolysaccharides which is most rapid during development and growth, and slow during ageing. This loss is mostly of hyaluronic acid, and there is a corresponding loss of water-holding capacity, while there is a relative or absolute increase in sulphated mucopolysaccharides. Detailed data for a specific example may be found in [31].

The interfibrillar matrix, then, is originally relatively rich in hyaluronic acid and relatively expanded because of its high water-holding capacity. The loss of hyaluronic acid would be expected to result in a reduced space-filling effect and contraction of the matrix, specifically of chondroitin sulphate which is strongly associated with collagen. Such a contraction could produce compressive stress on the collagen fibres, and the same conditions for co-operative fibre buckling as were created in the synthetic samples.

9. Conclusions

The model composite systems consisting of synthetic fibres buckled by shrinking the matrix material in which they are embedded show a pattern of major general similarities with the waveform ultrastructure found in rat tail tendon and other fibrous collagen tissues, specifically:

1. transmission polarizing microscopy shows that the wave shapes are clearly planar as opposed to helical, although the latter shape has been suggested for both materials in the past;

2. the wave shape in both cases deviates from a simple sine wave toward the shape of a planar zig-zag. This deviation is in the opposite direction from that seen in a buckled beam which is not laterally supported, indicating the effect of the surrounding matrix;

3. buckling of parallel multiple fibres is co-operative over quite large fibre separations, up to about 10 fibre diameters. In this range, fibres buckle in phase, with the wave shapes in parallel planes (co-planar, when possible, to the plane defined by the original fibre centrelines). These co-operative effects produce the same relations between individual fibres as seen in RTT, even for very low fibre volume fractions;

4. when strained beyond their respective elastic limits, both RTT and buckled synthetic fibres show the formation of a second waveform superimposed on the original, and of much smaller periodicity. In the synthetic models, this is due to slippage at the fibre-matrix interface as the sample is extended, and rebuckling of the fibre in the channel of matrix material as the sample is released.

In addition, the models offer information about the strains in the matrix surrounding the fibres, where corresponding information in the collagen tissues is not accessible.

This pattern of similarities suggests that fibre buckling can produce synthetic models for biological tissues which are useful, if only empirically. However, the available information about the ground substance mucopolysaccharides and the formation of collagen fibres also suggests a hypothetical mechanism for fibre buckling during the development of connective tissue, and that this is the cause of its ultrastructure.*

**Note added in proof.* We have recently observed that the collagen fibres of newborn (but not adult) RTT may straighten out spontaneously when the non-collagen matrix is digested enzymatically. This supports the idea that fibre buckling does occur during the formation of connective tissue, but leaves the mechanism still unclear. A report is in preparation.

Acknowledgements

The authors wish to thank Professor Andrew Keller for his advice and encouragement, and for access to the unpublished results of Gathercole, Keller and Shah. We also thank Professor Morton H. Litt for suggesting use of the polymerization shrinkage of ethyl acrylate to prepare the cylindrical samples, and Professor John K. Gillham for helpful discussions of thermoelastic fibre buckling. We appreciate the experimental assistance of Mr John A. Maksem and Mr Roger Duff in the difficult and tedious job of preparing the samples.

Financial support of the US National Institutes of Health under grants HD-00304-03 and HD-00669-13 is gratefully acknowledged.

References

1. D. H. ELLIOTT, *Biol. Rev.* **40** (1965) 392.
2. J. DIAMANT, A. KELLER, E. BAER, M. LITT and R. G. C. ARRIDGE, *Proc. Roy. Soc. Lond. B* **180** (1972) 293.
3. W. C. DALE, E. BAER, A. KELLER and R. R. KOHN, *Experentia* **28** (1972) 1293.
4. L. J. GATHERCOLE, A. KELLER and J. S. SHAH, submitted to *J. Microscopy*.
5. F. WASSERMAN, *Ergeb. Anat. Entw. Gesch.* **35** (1956) 240.
6. H. SOBEL, in "Advances in Gerontological Research" (edited by B. L. Strehler) (Academic Press, New York, 1967) (Vol. 2 pp. 205-283.
7. F. R. PARTINGTON and G. C. WOOD, *Biochim. Biophys. Acta* **69** (1963) 485.
8. S. M. BYCHKOV, S. S. NIKOLAEVA and V. N. KHARLAMOV, *Doklady Akad. Nauk. SSSR* **182** (1968) 1428. English translation, *Doklady Biochem.* **182** 243.
9. G. S. HOLLISTER and C. THOMAS, "Fibre Reinforced Materials" (Elsevier, London, 1966) Chapter 3.2.
10. L. J. BROUTMAN and R. H. KROCK, "Modern Composite Materials" (Addison Wesley, Reading, Mass., 1967) Chapter 2.5.
11. W. Y. CHUNG and R. B. TESTA, *J. Composite Mater.* **3** (1969) 58.
12. F. J. MCGARRY, *Trans. Inst. Chem. Eng.* **182** (1964) CE236.
13. J. K. GILLHAM, P. N. REITZ and M. J. DOYLE, *Polymer Eng. and Sci.* **8** (1968) 227.
14. R. V. SOUTHWELL, "Theory of Elasticity" (Clarendon Press, Oxford, 1936) Arts. 471-478.
15. S. TIMOSHENKO, "Theory of Elastic Stability" (McGraw-Hill, New York, 1936) Chapter II, Art. 21.
16. D. S. JACKSON and J. P. BENTLEY, in "Treatise on Collagen" Vol. 2 (edited by G. N. Ramachandran) (Academic Press, New York, 1968) Part A, Chapter 4.
17. R. ROSS, *ibid* Chapter 1.
18. B. P. TOOLE and D. A. LOWTHER, *Biochem J.* **109** (1968) 857.
19. A. F. FORZIATI, in "Analytical Chemistry of High Polymers" (edited by G. M. Kline) (Interscience, New York, 1962) Part II, Chapter 3.3.
20. S. FITTON JACKSON, *Proc. Roy. Soc. Lond. B* **144** (1956) 556.
21. B. J. RIGBY, N. HIRAI, J. D. SPIKES and H. EYRING, *J. Gen. Physiol.* **43** (1959) 265.
22. M. ABRAHAMS, *Med. and Biol. Eng.* **5** (1967) 433.
23. F. R. JOHNSON and R. M. H. MCMINN, *Biol. Rev.* **35** (1960) 364.
24. M. SCHUBERT and D. HAMERMAN, in "The Amino Sugars" Vol. IIA (edited by E. A. Balazs and R. W. Jeanloz) (Academic Press, New York, 1965) Chapter 31.
25. M. SCHUBERT and D. HAMERMAN, "A Primer on Connective Tissue Biochemistry" (Lea and Febiger, Philadelphia, 1968) Chapter 3.
26. M. B. MATTHEWS, *Biochem. J.* **96** (1965) 710.
27. L. ROSENBERG W. HELLMANN and A. K. KLEINSCHMIDT, *J. Biol. Chem.* **245** (1970) 4123.
28. R. A. GELMAN, W. B. RIPPON and J. BLACKWELL, *Biochem. Biophys. Res. Comm.* **48** (1972) 708.
29. R. A. GELMAN and J. BLACKWELL, *Conn. Tiss. Res.* **2** (1973).
30. T. C. LAURENT, in "Capillary Permeability (Proc. Alfred Benzon Symp. II (1969)" (edited by Christian Crone) (Munksgaard, Copenhagen, 1970) p. 261.
31. D. LOVELL, C. J. SHORAH and R. C. CURRAN, *Brit. J. Exp. Pathol.* **47** (1966) 228.

Received 21 August and accepted 22 August 1973.